Virchows Arch (2000) 437:667–674
DOI 10.1007/s004280000276

ORIGINAL ARTICLE

Mônica Gomes Pessanha
Carlos Alberto Mandarim-de-Lacerda

Influence of the chronic nitric oxide synthesis inhibition on cardiomyocytes number

Received: 2 February 2000 / Accepted: 21 June 2000 / Published online: 21 October 2000

Abstract This work analyzes the relationship between the number of viable cells and alteration of the cardiomyocytes growth response capacity of the hypertensive rat myocardium. Hypertension was induced in Wistar rats by means of nitric oxide synthesis blockade using N^G-nitro-L-arginine methyl ester (L-NAME). L-NAME (12 mg/kg per day) was given to animals in drinking water ad lib for 15 weeks. Proliferating cell nuclear antigen (PCNA) protein expression and the disector method were used to evaluate the proliferation capacity of the cardiomyocytes and its numerical density alteration (Nv[m]), respectively. Terminal deoxynucleotidyl transferase-mediated dUTP-biotin nick end labeling (TUNEL) and monoclonal antibody to single-stranded DNA were two methods that detected the process of the apoptotic cell death. The association of the p53 expression with the apoptosis was investigated using anti-p53 antibody. The heart weight, body weight, and heart weight/body weight ratio of the control rats increased 114%, 77%, and 22%, respectively, and the Nv[m] decreased 60% (P<0.0001) relative to the L-NAME rats. The cardiomyocytes did not present PCNA labeling, indicating the absence of cellular proliferation. The decline of the Nv[m] was also associated with apoptotic cell death in the myocardium of the hypertensive rats. A p53-dependent pathway seems to mediate the programmed cell death in this model of hypertension.

Keywords Apoptosis · Hyperplasia · Hypertension · Nitric oxide · Stereology

M. Gomes Pessanha (✉) · C.A. Mandarim-de-Lacerda
Laboratório de Morfometria, UERJ,
(Prof. Dr. C. A. Mandarim-de-Lacerda), Instituto de Biologia,
Centro Biomédico, Av. 28 de Setembro, 87 (fds),
20551–030 Rio de Janeiro, RJ, Brasil
e-mail: mgpessanha@hotmail.com
Tel.: +55-21-5876416

M. Gomes Pessanha
Department of Pathology, University Federal Fluminense, Brazil

Introduction

The effects of the overload pressure on human and animal hearts are characterized as a response of the myocyte and nonmyocyte components of the myocardium to preserve the cardiac performance [14, 37, 40, 41, 42]. Depending on the duration and nature of the hypertensive stimulus, myocardial structural changes can occur and constitute the basis for contractile impairment of the myocardium [20, 24, 58]. It is also possible that alterations in the molecular control of the cardiomyocyte hypertrophy are involved in this phenomenon [5, 18].

The pathogenetic mechanism responsible for the deterioration of myocardial function remains unclear, but it may be related to progressive intrinsic contractile dysfunction of residual viable cardiomyocytes and/or to ongoing degeneration and loss of cardiomyocytes [12, 49]. Multifocal areas of myofiber degeneration and fibrosis throughout the free wall of the left ventricle were described in the experimental hypertension using L-NAME (N^G-nitro-L-arginine methyl ester hydrochloride), but the etiology of cardiomyocyte loss in this model of hypertension remains unanswered [41, 42]. The current work speculates that the programmed cell death, besides the necrosis, may lead to progressive contractile dysfunction of residual cardiomyocytes.

Morphologically, programmed cell death is known as apoptosis and was first described by Kerr and coworkers [25]. It is a strategic biological and gene-regulated process of cell suicide that plays a crucial role in the development of multicellular organisms by eliminating unwanted cells associated with various degenerative, hyperproliferative, and autoimmune diseases [22, 60].

The process of DNA fragmentation, the key biochemical feature of apoptosis, is associated either with the abnormal expression of genes, such as Fas, ICE (interleukin-1B-converting enzyme), p53, and c-myc, or a deficiency of other genes, such as bcl2 [29]. The p53-stimulated transcription of the proapoptotic gene, bax, and repression of the antiapoptotic gene, bcl2, may elicit apoptosis [27]. Protein levels of p53 increase in response

to DNA damage, oxidative stress, and hypoxia. The expression of p53 plays an important role in regulating cell death in postmitotic cell populations [32].

DNA degradation, triggered by activation of an endogenous endonuclease, is specific to the spacer regions, leaving the DNA associated with the nucleosomes intact. This pattern of DNA cleavage can be detected morphologically by using the terminal deoxynucleotidyl transferase (TdT)-mediated dUTP-biotin nick end labeling assay (TUNEL) [13] and the monoclonal antibody to single-stranded DNA (mAB to ssDNA) method [10, 11].

Mature ventricular cardiomyocytes are considered to be terminally differentiated cells, but some indications suggest that the inability of cardiomyocytes to undergo mitotic division is a property that may be repressed and not irreversibly lost [7]. Potential candidates for this modulation are growth-related genes [48]. Experimental studies demonstrated that severe cardiac dysfunction could be associated with molecular adaptations in cardiomyocytes involving an upregulation of the message for two cell cycle-related genes, proliferating cell nuclear antigen (PCNA) and histone-H3 [47]. PCNA, a cofactor of DNA polymerase delta, is a late growth-regulated gene that is expressed at the G1-S boundary of the cell cycle [3, 6, 45, 46]. In normal mature ventricular cardiomyocytes, PCNA protein has not been demonstrated. However, in pathological states, characterized by severe ventricular dysfunction and failure, the expression of PCNA mRNA is markedly enhanced in association with the appearance of PCNA protein in the stressed cardiomyocytes [47, 48].

The phenomenon of cardiomyocyte loss, in segmental, focal, or diffuse patterns, complicates the analysis of the magnitude of reactive growth in the ventricular myocardium [2]. Thus, an association between stereological and immunohistochemical methods would be of significant scientific value to identify changes in the replicatory machinery of cardiomyocytes and/or their cell death during the hypertension by nitric oxide (NO) synthesis inhibition.

Material and methods

Animals

Both male and female Wistar rats were used in the study. In the beginning of the experiments, the animals were 16 weeks old. The injured tissue was taken from 14 hypertensive animals (seven females and seven males) that received normal rat chow (Purina) and NO synthase inhibitor in their drinking water (L-NAME, 12 mg/kg per day; Sigma Co, Lot 44H0102) for 15 weeks. Normal tissue was taken from ten other animals (five females and five males) that received only normal chow and drinking water ad lib for 15 weeks. Tail blood pressure was measured before and during the experiment using tail cuff plethysmography (RTBP1007; Kent Scientific Co., Litchfield, Conn., USA). Before sacrifice, animals were anesthetized with ether inhalation. The heart was exposed, and a great volume of KCl (10%) was injected into the left ventricle as a cardioplegic solution, which stops the heart in diastole. Fragments of the free left ventricular wall were fixed through immersion in 10% buffered formalin pH 7.2, for at least 6 h at room temperature and then prepared for histological and immunohistochemical studies. The fragments were embedded in paraffin and 5-µm-thick sections were prepared.

Immunohistochemistry

Double immunohistochemistry for PCNA and α-sarcomeric actin

The immunohistochemical analysis used a modification of the immunoperoxidase method [19]. To investigate whether PCNA protein labeling occurred in adult ventricular cardiomyocyte nuclei, double labeling of PCNA and α-sarcomeric actin was performed. Paraffin sections (3-µm thick) were attached to aminoalkylsilane-treated slices and deparaffinized. The intrinsic peroxidase activity was inhibited by the addition of 10% H_2O_2 in 70% methanol for 10 min. Subsequently, the sections were incubated in 1% skimmed milk solution for 1 h to quench nonspecific protein binding. Paraffin sections were incubated for 50 min at room temperature with monoclonal mouse antibody anti-PCNA (M0879; Dako), which was diluted 1:200 in Tris-buffered saline (TBS) plus 1% bovine serum albumin. After being washed with TBS, the sections were incubated for 30 min at room temperature with rabbit anti-mouse biotinylated secondary antibody (E0354; Dako), which was diluted 1:200. Furthermore, the sections were incubated with alkaline phosphatase-mouse anti-alkaline phosphatase immune complex (double stain kit system 40/K665 Dako) for 30 min at room temperature. After the final washing with TBS, fast red chromogen (K597; Dako) was used as a chromogen to visualize the immunoreactivity. After extensive washing with TBS, nonspecific antigens were blocked by incubation of the sections in 1% skimmed milk solution for 1 h at room temperature. Subsequently, the sections were incubated overnight with monoclonal anti-α-sarcomeric actin antibody (M0874; Dako), which was diluted 1:200 in TBS plus 1% bovine serum albumin. After being washed with TBS, the sections were incubated with the same biotinylated secondary antibody used for PCNA labeling. The sections were then incubated for 40 min at room temperature with streptavidin–biotin–horseradish peroxidase (Strept AB complexes K0377; Dako) which was prepared according to the manufacture's instructions. After the final washing with TBS, 0.1% 3.3-diaminobenzidine tetrahydrochloride (5 mg; Sigma) in 10 ml of TBS buffer, pH 7.0, containing 200 µl of 10% H_2O_2 was used as a chromogen to visualize the immunoreactivity. Sections without primary antibodies were used as negative controls. As positive controls for PCNA and α-sarcomeric actin, rat skin and the hearts of the control rat, respectively, were used. Before mounting, the sections were lightly counterstained with Mayer's hematoxylin, dehydrated, and mounted with glycerol.

Immunohistochemistry for p53

A mouse monoclonal antibody against human p53 protein (M7001; Dako) as the primary antibody was used for p53 immunohistochemical staining. The deparaffinized thin sections were twice treated using microwave irradiation at 500 W for 5 min in 10 mM citrate buffer, pH 6.0. Endogenous peroxidase was quenched by the addition of 10% H_2O_2 in 70% methanol for 10 min. Subsequently, the sections were incubated in 1% skimmed milk solution for 1 h to quench nonspecific protein binding. The sections were then incubated for 1 h at room temperature in antibody anti-p53, which was diluted 1:200. Thereafter, the sections were incubated for 30 min at room temperature with a rabbit anti-mouse biotinylated secondary antibody (E0354; Dako) which was diluted 1:200. Furthermore, the sections were incubated for 40 min at room temperature with streptavidin–biotin–horseradish peroxidase (Strept AB complexes K0377; Dako) which was prepared according to the manufacture's instructions. Sections were then stained with 0.1% 3.3-diaminobenzidine tetrahydrochloride (5 mg; Sigma) in 10 ml of TBS buffer, pH 7.0, containing 200 µl of 10% H_2O_2. The slides were washed with TBS between all steps,

except before incubation in the primary antibody. Before mounting, the sections were lightly counterstained with Mayer's hematoxylin, dehydrated, and mounted.

Detection of apoptosis

TUNEL technique

The staining was performed according to Gavrieli and coworkers [13]. The hearts were fixed in 10% neutral buffered formalin (4% formaldehyde), embedded in paraffin, and sectioned. Deparaffinized and rehydrated sections were treated with 2% H_2O_2 in TBS to quench endogenous peroxidase and then stained with the in situ apoptosis detection kit (Oncor ApopTag, Gaithersburg). This method uses the TUNEL technique [13]. The sections were incubated with 20 µg/ml proteinase K for 15 min at room temperature. Subsequently, the sections were immersed in equilibration buffer for 30 min at room temperature and then incubated in a solution of TdT at 37°C for 1 h in a humid chamber. At 37°C for 20 min at room temperature, stop/wash buffer solution was used to stop the reaction. After extensive washing in TBS, the sections were incubated with anti-digoxigenin-peroxidase solution in a humid chamber for 30 min at room temperature. 3,3-diaminobenzidine tetrahydrochloride (0.1%) was used as a chromogen. The intensity of immunohistochemical staining was monitored continuously using light microscopy to confirm optimal sensitivity of the assay. The incubation time was controlled according to the first appearance of positivity in the positive control provided by the manufacturers of the kit. The sections were lightly counterstained with methyl green, washed with distilled water, treated with butanol, immersed in xylene, and mounted. Sections of mammary gland provided by the manufacturer were used as positive controls. Negative controls were prepared by replacing TdT enzyme with distilled water.

mAB to ssDNA

The detection of apoptotic cells with mABs has been previously described [10, 11]. Tissues were fixed in 10% neutral buffered formalin (4% formaldehyde), dehydrated in xylene, and embedded in paraffin. Deparaffinized and rehydrated sections were treated with 2% H_2O_2 in TBS to quench endogenous peroxidase. Sections of 3 µm were subsequently treated with 0.1 N HCl for 10 min at room temperature. After being washed with TBS, the sections were resuspended in TBS supplemented with 5.0 mM $MgCl_2$, heated in a water bath at 100°C for 5 min, and cooled on ice. The sections were washed with TBS and then treated with 1% skimmed milk solution for 1 h at room temperature. Furthermore, the sections were incubated for 50 min with mAB to ssDNA (M3299, Chemicon), which was diluted 1:50. After being washed with TBS, the sections were incubated for 30 min at room temperature with a rabbit anti-mouse biotinylated secondary antibody (E0354; Dako), which was diluted 1:200. The sections were then incubated for 40 min at room temperature with streptavidin–biotin–horseradish peroxidase (Strept AB complexes K0377; Dako), which was prepared according to the manufacture's instructions. Diaminobenzidine (DAB) was used as a chromogen. Before mounting, the sections were lightly counterstained with Mayer's hematoxylin, dehydrated, and mounted.

Stereology

The heart volume and the volume of the ventricles were determined according to the submersion method of Scherle [52], in which the water displacement due to organ volume is recorded by weight. The organ was suspended on a stand by a thin thread and immersed in physiologic solution in a recipient on the plate of the scale without touching the walls of the recipient. On the day of the sacrifice, the heart weight/body weight ratio (HBR) was determined as HBR=(HM/BM).100(%).

After this, hearts were fixed in buffered formalin (10%, pH 7.2) for at least 6 h at room temperature. To generate appropriated sections for stereological study, the hearts were sectioned in an isotropic uniform random set of three perpendicular sections for each heart analyzed [an orthogonal triplet probe (ortrip)] [36]. The left ventricle was dissected and cut with the cut edge down and, at random, the specimen was cut with a section perpendicular to the first plane. After this, it was placed with the new cut surface down and a new random orientation was defined with the organ being sectioned perpendicular to the previous plane. The last cut was considered to be uniformly isotropic [35].

Stereology was performed using ten random microscopic fields, oil-immersion ×100 objective, and video microscopy (Leica model DMRBE). The counts used an M42 test system put upon the screen of the monitor and calibrated with a Leitz micrometer 1 mm/100.

The disector method was used to obtain the numerical density of the cardiomyocytes [53]. The optical disector is based on section pairs and is constructed with two parallel sections separated by one section thickness (lookup and lookdown planes). These planes were determined over a frame of known surface [17]. Light microscopic fields were selected in a systematic random manner from reference sections. We sampled all cardiomyocytes nuclei seen in focus only in the lookup plane. They should be partly or totally inside the frame provided they did not in any way intersect the left or inferior exclusion edges or their extensions ("forbidden line") [16].

The numerical density of the cardiomyocytes (number of cardiomyocytes per volume of myocardium, Nv[m] 1/mm^3) was determined with ten random disector pairs for each specimen [17]. For reasons of efficiency, one nucleus was considered to represent one cardiomyocyte. Q_A is the number of the cardiomyocyte nuclei in the test area appearing in an unbiased counting frame of 4200.0 µm^2 on the one-slice plane. The volume disector is the product of the disector thickness (t) by the test-area (A_T).

$$Nv[m] = \frac{Q_A^-}{t.A_T} 1/mm^3.$$

Statistical analysis

Differences in the blood pressure between control and L-NAME groups were tested with the Student's *t*-test. Differences in stereological parameters were estimated using the Mann-Whitney U test. A *P* value below 0.05 was considered significant [62].

Results

The tail blood pressure was significantly different between control and L-NAME rats after the fourth week of L-NAME administration (Table 1). In control animals, no variation in tail blood pressure was noted during the experimentation; however, in L-NAME rats, it reached 150 mmHg at the 13th week.

PCNA labeling of the ventricular myocardium

The distribution of PCNA protein in the myocardium was detected using the immunoperoxidase technique. PCNA labeling was not observed in the cardiomyocytes surrounding the lesion area in the L-NAME myocardium, but labeling in the nuclei of the nonmyocyte cells of the left ventricle of L-NAME hearts was detected, especially in the lesion areas (Fig. 1a).

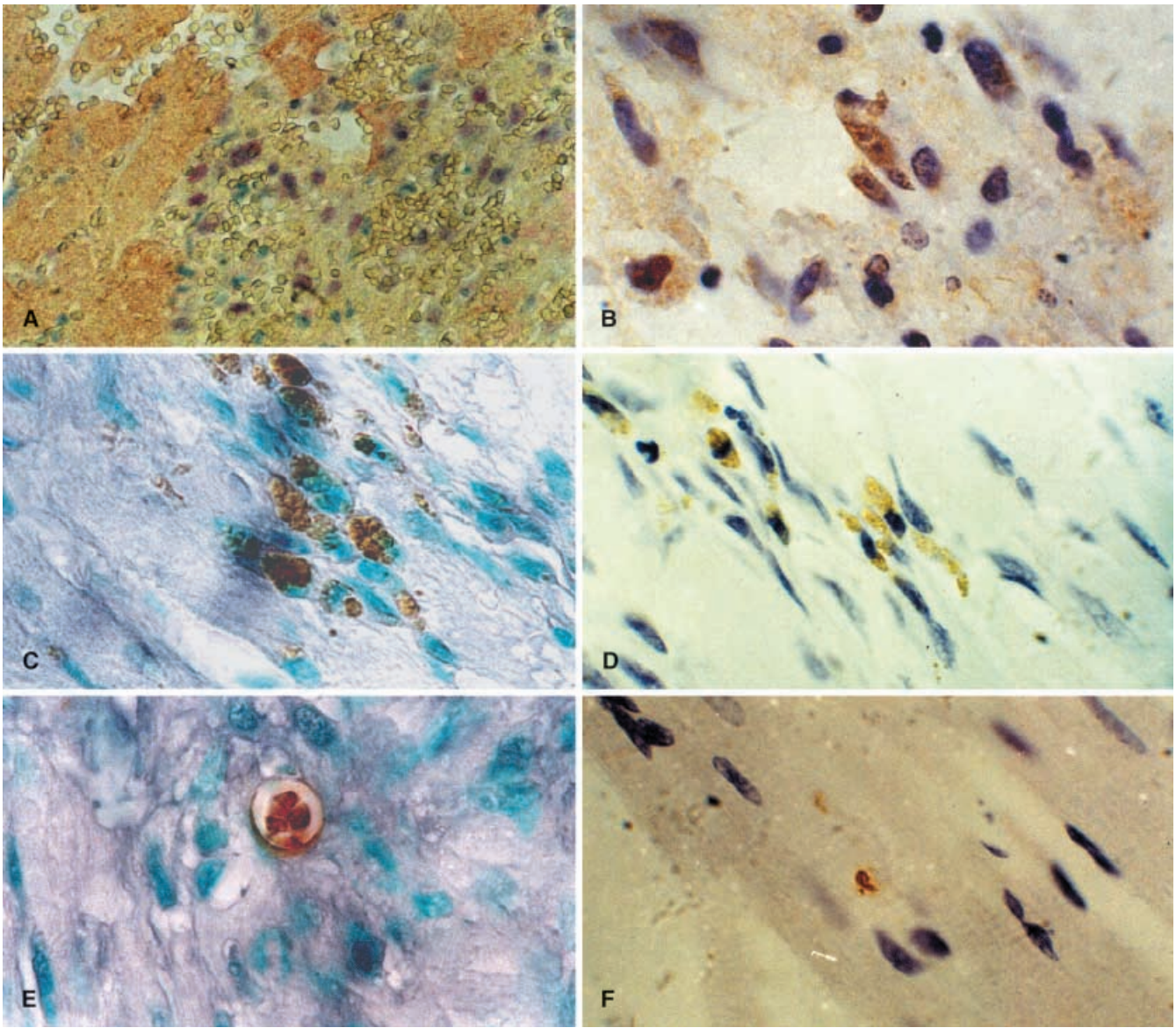

Fig. 1 Photomicrographs of the myocardium in N^{G}-nitro-L-arginine methyl ester (L-NAME) rats. **A** Double staining of proliferating cell nuclear antigen (PCNA) and sarcomeric actin in lesion area presenting neighboring hypertrophied cardiomyocytes and an absence of labeled nuclei of cardiomyocytes stained positively with sarcomeric actin (*arrowheads*; ×170). **B** Immunohistochemical findings of p53 protein. Inflammatory cells infiltrating into the lesion areas showed dark-brown positive immunoreactivity against anti-p53 protein antibody (*arrows*), the majority of cardiomyocytes were negative (*arrowhead*; ×350). **C, D** Some apoptotic inflammatory cells were found within lesion areas using both terminal deoxynucleotidyl transferase-mediated dUTP-biotin nick end labeling (TUNEL) and monoclonal antibody (mAB) methods, respectively (*arrows*; ×350). **E** Single apoptotic cell presenting fragmented nucleus with appearance of cloverleaf (*arrow*; ×350). **F** In a relatively early stage, in which there is not a formation of blebbing, it is possible to identify the origin of the cells from their morphological appearance. The *arrow* probably indicates the nucleus of an apoptotic cardiomyocyte presenting its typical cytoplasmatic striation in mAB method (×350)

Table 1 The tail blood pressure (mean ±SD) in control and N^{G}-nitro-L-arginine methyl ester (L-NAME) rats during the study. *P* probability that the differences between groups were significant, Student's *t*-test; *NS* significant

Weeks	Control	L-NAME	*P*
Before L-NAME administration	99.4±1.0	99.6±1.7	NS
After L-NAME administration			
4th	99.5±0.7	114.5±1.3	<0.0001
8th	99.9±0.3	127.9±2.6	<0.0001
10th	100.8±0.5	142.9±2.6	<0.0001
13th	101.0±2.1	150.0±1.8	<0.0001
14th	101.5±2.4	150.0±2.1	<0.0001
15th	102.5±2.6	150.0±2.2	<0.0001

p53 immunostaining

The myocardium of the hypertensive rats presented dark-brown immunoreactivity to p53 protein (Fig. 1b). Several inflammatory cells within the lesion areas showed

Table 2 Quantitative analysis of the myocardium in control and N^G-nitro-L-arginine methyl ester (L-NAME) groups. *Nv[m]* numerical density of the myocytes, *N[m]* total number of myocytes in the heart, *HW* heart weight, *BW* body weight, *HBR* heart weight/body weight ratio, *CI* confidence interval at 95%, *CE* coefficient of error calculated as SE/mean, *CV* coefficient of variaton, *P* probability of the difference between control and L-NAME groups are significant (Mann-Whitney test)

Groups	Nv[m] $10^4/mm^3$	N[m] (10^7)	HBR (%)	HW (g)	BW (g)
Control					
Median	27.7	24.3	0.54	0.9	168.2
CI (95%)	26.9–28.5	22.3–26.2	0.53–0.56	0.8–0.9	150.6–173.8
CV %	4.0	11.2	3.8	9.0	10.0
CE %	1.3	3.6	1.2	2.8	3.2
L-NAME					
Median	10.3	20.9	0.67	1.9	291.3
CI (95%)	10.1–12.0	18.8 to 22.9	0.64–0.69	1.8–2.0	266.2–306.4
CV %	15.1	16.8	6.6	6.5	12.1
CE %	4.0	4.5	1.8	1.7	3.2
P	0.00004	0.02	0.00004	0.00003	0.00004

positive p53 immunoreactivity. There was no evidence of positive p53 immunoreactivity in the cardiomyocytes and interstitial cells in the areas that did not present a lesion in the myocardium of the L-NAME group. In the L-NAME group, there was positive p53 immunoreactivity in the nuclei of the little cardiomyocytes surrounding the lesion areas. However, dead cardiomyocytes within lesion areas showed no positive immunoreactivity. There were no findings of positive immunoreactivity in the myocardium of the control group.

Apoptosis detected using the TUNEL and mAB to ssDNA methods

Apoptotic cells stained with TUNEL and mAB methods were mainly observed in the inflammatory cells (Fig. 1c,d). Rare apoptotic cardiomyocytes were observed scattered in the myocardium of the L-NAME rats with both of these methods. The presence of the cellular striation in the cells presenting apoptotic nuclei indicates that these cells probably represent the cardiomyocytes in the early stages of apoptosis. Apoptotic bodies can be observed in the myocardium of the L-NAME rats and possibly represent later stages of apoptosis. Figure 1e illustrates the originally described morphological feature of the apoptosis, the nuclear fragmentation originating blebbing, similar to a cloverleaf, only observed with the TUNEL method. No detectable apoptosis was seen in the myocardium of the control group using either method.

Quantitative analysis

The differences between control rats and L-NAME rats were significant ($P<0.0001$). The results are expressed as median and confidence interval (CI) at 95%. Comparing the myocardium in control and L-NAME groups, the body weight increased 77%, and the heart weight increased 114%. The HBR in the L-NAME group increased 22%. Both Nv[m] and N[m]decreased 60% and 14%, respectively (Table 2). There was no difference between genders.

Discussion

The consequences of the chronic inhibition of NO biosynthesis on myocardial structures have yet to be studied [37, 40, 54]. The present results provide some evidence that the chronic NO synthesis inhibition participates in the decrease of the cardiomyocytes number. Moreno and co-workers [37] compared the myocardial alterations in hypertensive rats using the chronic inhibition of NO biosynthesis (utilizing L-NAME) with those having renal hypertension (Goldblatt II model 2K1C). Both groups of rats had a similar high blood pressure level. The L-NAME-treated rats showed significantly more severe and extensive cardiac lesions than the 2K1C ones. Moreover, the authors observed that rats treated with the inactive enantiomer D-NAME had no increase in the blood pressure and did not present myocardial lesions, suggesting that these lesions are related to the inhibition of NO biosynthesis [37].

Myofiber hypertrophy is the prevailing form of cardiomyocyte growth in the hypertensive rat heart that received L-NAME for 25 days [40]. Both hypertrophy and hyperplasia processes occur in different cardiac disease states [38, 39, 46]. However, the magnitude of reactive growth in the ventricular myocardium could be complicated by the phenomenon of cardiomyocyte loss [46].

The HBR corrects the heart mass considering the size of the animals, and normally is unchanged during aging, except in very old rats and in humans older than 85 years [31]. In the present study, the HBR values demonstrated a significant increase in the heart mass of the L-NAME group caused by NO synthesis inhibition and hypertension. When the results are not normalized for the body mass, the degree of hypertrophy is always more pronounced on the left side than on the right one [34]. However, the decline of the Nv[m] and of the N[m] suggests that if cardiomyocyte proliferation occurs as demonstrated by some studies on cardiac failure [21, 39, 46], the rate of cardiomyocytes loss seems to be higher than the rate of the cardiomyocyte proliferation in the L-NAME model of the experimental hypertension.

In ventricular cardiomyocytes of different animals, including man, DNA replication, ploidy formation, and

multinucleation are present in normal and pathologic states [21, 46, 47, 48], and this could lead to inconsistencies in the determination of Nv[m]. However, the optical disector permits the definition within the thickness of the section, avoiding the over-counting of binucleated cells. If the section thickness is known, it is possible to observe the nuclei in the middle of the section and use the rest of the thickness to ensure that sampling was unique and uniform [17].

Cardiac hypertrophy is associated with the reexpression of the atrial natriuretic factor gene in ventricular cardiomyocytes [9]. Defects of the molecular control of cardiomyocyte hypertrophy per se or associated cardiomyocyte loss should affect the adaptive mechanism of the cardiac hypertrophy by decreasing the number of viable cells and by alteration of their growth response capacity. Consequently, the cardiomyocytes may reexpress their capacity to synthesize DNA and undergo cell division such as it occurs in the hypertrophic senescent heart in humans [38].

Cardiomyocyte hyperplasia by definition implies an increase in the number of ventricular muscle cells. Numerical density analysis can detect an increase or decrease of cells but not simultaneous cellular loss and proliferation [47]. Other techniques are necessary to identify if cardiomyocytes reexpress their ability to synthesize DNA and proliferate [46]. In this study, the presence of PCNA in the cardiomyocyte nuclei was associated with the Nv[m] determination to overcome this difficulty. The cardiac failure is characterized by a significant increase in ventricular cardiomyocytes PCNA protein [47, 48]. Cardiomyocytes of both control and L-NAME rats in this study did not show PCNA protein expression, but the Nv[m] was significantly lower in L-NAME rats than in control ones of the same age. This suggests that the concept that the cardiomyocyte cellular hyperplasia can be induced in mature differentiated cardiac muscle cells in pathologic conditions is not applied to this hypertension model.

In the myocardium of the hypertensive rats, inflammatory infiltrate cells presented PCNA labeling. This is not surprising in view of previous works that demonstrated intense proliferation of interstitial and endothelial cells and myofibroblasts during the evolution of inflammatory process [43, 57, 59]. PCNA interpretation is made difficult because of their long half-lives, which lead to persistence of staining even in cells that have recently left their proliferation capacity. In the future, other markers of cellular proliferation, such as Ki-67, could be required for this purpose, because they seem to offer fewer limitations than PCNA [61].

The decrease of the Nv[m] observed in the present study is predominantly due to the death of cardiomyocytes, and experiments in various animals models indicated that both apoptotic and necrotic mechanisms can occur [32]. The observation of the cell death by apoptosis was provided by the data from the mAB to ssDNA and TUNEL assays. The TUNEL method has been severely misleading for the evaluation of the cell death mechanism, because it stains both necrotic and apoptotic cells indistinctly [1, 10]. The TUNEL method seems to be satisfactory for identifying apoptotic cells in the myocardium, but the better sensibility of the mAB to ssDNA assay compared with TUNEL for this identification is not discarded.

The present results suggest that, besides necrosis, apoptosis of the cardiomyocytes also seems to have mediated the cardiomyocyte cellularity decrease in the experimental hypertension induced by L-NAME. Double immunohistochemistry for the apoptotic method and cell-specific proteins might permit differentiation of the nature of the apoptotic cells. However, it could be invalid in later stage apoptotic cells characterized by the bleb formations that detach into apoptotic bodies [30, 49].

The apoptosis might be related to the disappearance of infiltrating cells at the chronic stage of inflammation [50, 51]. In addition, cytotoxic inflammatory infiltrate cells might be removed by apoptosis to avoid releasing of their cellular contents and thus to prevent prolonged inflammation [55]. In this study, the cells in later stages of apoptosis could represent cardiomyocytes salvaged into lesion areas or remaining macrophages. In this case, macrophage death by apoptosis would be a beneficial mechanism in areas that present some remodeling degree, avoiding cellular content to be released and induce an inflammatory process in fibrotic tissue.

Apoptosis was induced by p53 in cardiomyocytes and inflammatory cells. This cellular adaptation seems to also be associated with the decline of the numerical density of the cardiomyocytes observed in hypertension induced by L-NAME. Previous studies demonstrated that independent mechanisms other than p53 are involved in the apoptotic pathway of cardiomyocytes [4, 26, 28, 32, 56].

Depending on the cell type, the increase in p53 protein levels or transactivating ability, which occurs in response to DNA damage, can result in either growth arrest or apoptosis [23, 33]. However, studies on the role of p53 in the regulation of programmed cell death have been almost exclusively confined to active proliferating cells [32].

The expression of p53 in cells that are capable of extensive proliferation, such as inflammatory cells, and in cells that are not capable of extensive proliferation, such as the cardiomyocytes, activates regulatory molecules that are associated with characteristic roles of these cells. It is still unclear what the signaling pathway that regulates the preferential expression of each of these molecules in target cells is [32, 44]. It is possible that the stimulus nature could be associated with deregulation of the cell cycle and thus, induction of the preferential expression of the cell cycle-dependent molecules.

The NO function and myocardial remodeling is still a subject under discussion. High amounts of NO are linked to proapoptotic effects under pathophysiological conditions, whereas the continuous release of endothelial NO inhibits apoptosis and may contribute to the antiatherosclerotic functions of NO [8]. NO interacts with estrogen

to modulate the apoptotic pathway in cardiomyocytes [15]. The present work examined some aspects of the NO biosynthesis inhibition causing hypertension and cardiomyocytes apoptosis. The presence of inflammatory cells and cardiomyocytes with positive p53 immunoreactivity suggests that this protein may play an important role on the apoptosis of these cells in the hypertension induced by L-NAME. The decrease of the Nv[m] with the absence of cardiomyocyte PCNA labeling suggests that cardiomyocyte hyperplasia did not constitute the dominant growth mechanism in hypertension caused by L-NAME administration. Further studies, however, are required to characterize the association between NO and cardiomyocyte apoptosis.

Acknowledgements This work was partially supported by the Brazilian agencies CNPq (146013/99–9 and 524114/97–0) and FAPERJ (170.770/98 and 151.495/99).

References

1. Ansari B, Coates PJ, Greenstein BD, Hall PA (1993) In situ end-labelling detects DNA strand breaks in apoptosis and other physiological and pathological states. J Pathol 170:1–8
2. Anversa P, Kajstura J, Cheng W, Reiss K, Cigola E, Olivetti G (1996) Insulin-like growth factor-1 and myocyte growth: the danger of a dogma. Part II. Induced myocardial growth: pathologic hypertrophy. Cardiovasc Res 32:484–495
3. Barsega R, Rubin R (1993) Cell cycle and growth control. Crit Rev Eukaryot Gene Expr 3:47–61
4. Bialik S, Geenen DL, Sasson IE, Cheng R, Horner JW, Evans SM, Lord EM, Koch CJ, Kitsis RN (1997) Myocyte apoptosis during acute myocardial infarction in the mouse localizes to hypoxic regions but occurs independently of p53. J Clin Invest 100:1363–1372
5. Bilsen MV, Chien KR (1993) Growth and hypertrophy of the heart: towards an understanding of cardiac specific and inducible gene expression. Cardiovasc Res 27:1140–1149
6. Bravo R, Frank R, Blundell PA, MacDonald-Bravo H (1987) Cyclin/PCNA is the auxiliary protein of DNA polymerase delta. Nature 326:515–517
7. Cummins P (1993) Fibroblast and transforming growth factor expression in the cardiac myocyte. Cardiovasc Res 27:1150–1154
8. Dimmeler S, Zeiher AM (1997) Nitric oxide and apoptosis: another paradigm for the double –edged role of nitric oxide. Nitric Oxide 1:275–281
9. Drexler H, Hänze J, Finckh M, Lu W, Just H, Lang RE (1989) Atrial natriuretic peptide in a rat model of cardiac failure: atrial and ventricular mRNA, atrial content, plasma levels, and effect of volume loading. Circulation 79:620–633
10. Frankfurt OS, Robb JA, Sugarbaker EV, Villa L (1996) Monoclonal antibody to single-stranded DNA is a specific and sensitive cellular marker of apoptosis. Exp Cell Res 226:387–397
11. Frankfurt OS, Robb JA, Sugarbaker EV, Villa L (1997) Apoptosis in breast carcinomas detected with monoclonal antibody to single-stranded DNA: relation to bcl2 expression, hormone receptors, and lymph node metastases. Clin Cancer Res 3: 465–471
12. Freude B, Masters TN, Kostin S, Robicsek F, Schaper J (1998) Cardiomyocyte apoptosis in acute and chronic conditions. Basic Res Cardiol 93:85–89
13. Gavrieli Y, Sherman Y, Ben-Sasson SA (1992) Identification of programmed cell death in situ via specific labeling of nuclear DNA fragmentation. J Cell Biol 119:493–501
14. Grimm D, Kromer EP, Böcker W, Bruckschlegel G, Holmer SR, Riegger GAJ, Schunkert H (1998) Regulation of extracellular matrix proteins in pressure-overload cardiac hypertrophy: effects of angiotensin converting enzyme inhibition. J Hypertens 16:1345–1355
15. Grohé C, Meye R, Vetter H (2000) Estrogens and the prevention of cardiac apoptosis. In: Schunkert H, Riegger GAJ (eds) Apoptosis in cardiac biology. Kluwer, Boston, pp 329–336
16. Gundersen HJG (1977) Notes on the estimation of the numerical density of arbitrary profiles: the edge effect. J Microsc 111:219–227
17. Gundersen HJG, Bagger P, Bendtsen TF, Evans SM, Korbo L, Marcussen N, Muller A, Nielsen K, Nyengaard JR, Pakkenberg G, Sorensen FB, Vesterby A, West MJ (1988) The new sterological tools: disector, fractionator, nucleator and point sampled intercepts and their use in pathological research and diagnosis. APMIS 96:857–881
18. Hefti MA, Harder BA, Eppenberger HM, Schaub MC (1997) Signaling pathways in cardiac myocyte hypertrophy. J Mol Cell Cardiol 29:2873–2892
19. Hsu SM, Raine I, Fanger H (1981) Use of avidin-biotin-peroxidase complex (ABC) in immunoperoxidase techniques. J Histochem Cytochem 29:577–580
20. Kahan T (1998) The importance of left ventricular hypertrophy in human hypertension. J Hypertens 16[suppl 7]:S23–S29
21. Kajistura J, Zhang X, Reiss K, Szoke E, Li P, Lagrasta C, Cheng W, Darzynkiewicz Z, Olivetti G, Anversa P (1994) Myocyte cellular hyperplasia and myocyte cellular hypertrophy contribute to chronic ventricular remodeling in coronary artery narrowing-induced cadiomyopathy in rats. Circ Res 74:383–400
22. Kajstura J, Cheng W, Ranganathan S, Li P, Li B, Nithahara JA, Chapnick S, Reiss K, Olivetti G, Anversa P (1996) Necrotic and apoptotic myocyte cell death in the aging heart of Fisher 344 rats. Am J Physiol 271:H1215–H1228
23. Kastan MB, Zhan Q, El-Deiry WS, Carrier F, Jacks T, Walsh WV, Plunkett BS, Vogelstein B, Fornace AJ (1992) A mammalian cell cycle chekpoint pathway utilizing p53 and GADD45 is defective in ataxia-telangiectasia. Cell. 13:587–597
24. Katz AM (1994) The cardiomyopathy of overload: an unnatural growth response in the hypertrophied heart. Ann Intern Med 121:363–371
25. Kerr JFR, Wyllie AH, Currie AR (1972) Apoptosis: basic biological phenomenon with wide-ranging implications in tissue kinetics. Br J Cancer 26:239–257
26. Kiess W, Gallaher B (1998) Hormonal control of programmed cell death/ apoptosis. Eur J Endocrinol 138:482–491
27. Kirshenbaum LA, Moissac D (1997) The bcl-2 gene product prevents programmed cell death of ventricular myocytes. Circulation 96:1580–1585
28. Leri A, Caludio PP, Li Q, Wang X, Reiss K, Wang S, Malhotra A, Kajstura A, Anversa P (1998) Stretch-mediated release of angiotensin II induces myocyte apoptosis by activating p53 that enhances the local renin angiotensin-system and decreases the Bcl2 to Bax protein ratio in the cell. J Clin Invest 101:1326–1342
29. Li D, Tomson K, Yang B, Mehta P, Croker BP, Mehta JL (1999) Modulation of constitutive nitric oxide synthase, bcl-2 and Fas expression in culturesd human coronary endothelial cells exposed to anoxia-reoxygenation and angiotensin II: role of AT1 receptor activation. Cardiovasc Res 41:109–115
30. Li Z, Bing OHL, Long X, Robinson KG, Lakatta EG (1997) Increased cardiomyocyte apoptosis during the transition to heart failure in the spontaneously hypertensive rat. Am J Physiol 272:H2313-H2319
31. Linzinzbach AJ (1960) Heart failure from the point of view of quantitative anatomy. Am J Cardiol 5, 370–382
32. Long X, Boluyt MO, Hipolito ML, Lundberg MS, Zheng J-S, O'Neill L, Cirielli C, Lakatta EG, Crow MT (1997) p53 and the hypoxia-induced apoptosis of cultured neonatal rat cardiac myocytes. J Clin Invest 99:2635–2643
33. Lowe SW, Schmitt EM, Smith SW, Osborne BA, Jacks T (1993) p53 is required for radiation-induced apoptosis in mouse thymocytes. Nature 362:847–849

34. Mallat Z, Swynghedauw B (2000) Molecular mechanisms of cardiac myocardial remodeling during aging. Role of apoptosis. In: Schunkert H, Riegger GAJ (eds) Apoptosis in cardiac biology. Kluwer, Boston, pp 273–286
35. Mandarim-de-Lacerda CA (1998) Stereology in the normal and pathological morphologic research. Biomed Res 9:153–163
36. Mattfeldt T, MøBius HJ, Mall G (1985) Orthogonal triplet probes: an efficient method for unbiased estimation of length and surface of objects with unknown orientation in space. J Micros 139:279–289
37. Moreno H, Metze K, Bento AC, Antunes E, Zatz R, Nucci G (1996) Chronic nitric oxide inhibition as a model of hypertensive heart muscle disease. Basic Res Cardiol 91:248–255
38. Olivetti G, Melissari M, Balbi T, Quaini F, Sonnenblick EH, Anversa P (1994) Myocyte nuclear and possible cellular hyperplasia contribute to ventricular remodeling in the hypertrophic senescent heart in humans. JACC 24:140–149
39. Olivetti G, Cigola E, Maestri R, Corradi D, Lagrasta C, Gambert SR, Anversa P (1996) Aging, cardiac hypertrophy and ishemic cardiomyopathy do not affect the proportion of mononucleated and multinucleated myocytes in the human heart. J Mol Cell Cardiol 28:1463–1477
40. Pereira LMM, Mandarim-de-Lacerda CA (1998) Quantitative examination of the cardiac myocytes in hypertensive rats under chronic inhibition of nitric oxide synthesis. J Biomed Sci 5:363–369
41. Pereira MMP, Vianna GMM, Mandarim-de-Lacerda CA (1998) Stereology of the myocardium in hypertensive rats. Differences in relation to the time of inhibition of nitric oxide synthesis. Virchows Arch 433:369–373
42. Pessanha MG, Mandarim-de-Lacerda CA, Hahn MD (1999) Stereology and immunohistochemistry of the myocardium in experimental hypertension: long-term and low-dosage administration of inhibitor of the nitric oxide synthesis. Pathobiol 67:26–33
43. Pessanha MG, Mandarim-de-Lacerda CA (2000) Healing rat myocardial and myofibroblast accumulation. Exp Toxicol Pathol 52:192–194
44. Pierzchalski P, Reiss K, Cheng W, Corrado C, Kajstura J, Nitahara JA, Rizk M, Capogrossi MC, Anversa P (1997) p53 induces myocyte apoptosis via the activation of the renin-angiotensin system. Exp Cell Res 234:57–65
45. Prelich G, Tan CK, Kostura M, Mathews MB, So AG, Downey KM, Stillman B (1987) Functional identify of proliferating cell nuclear antigen and a DNA polymerase-delta auxiliary protein. Nature 26:517–520
46. Quaini F, Cigola E, Lagrasta C, Saccani G, Quaini E, Rossi C, Olivetti G, Anversa P (1994) End-stage cardiac failure in humans is coupled with the induction of proliferating cell nuclear antigen and nuclear mitotic division in ventricular myocytes. Circ Res 75:1050–1063
47. Reiss K, Kajstura J, Capasso JM, Marino TA, Anversa P (1993) Impairment of myocyte contractility following coronary artery narrowing is associated with activation of the myocyte IGF-1 autocrine system, enhanced expression of late growth related genes, DNA-synthesis and myocyte nuclear mitotic division in rats. Exp Cell Res 207:348–360
48. Reiss K, Kajistura J, Zhang X, Li P, Szoke E, Olivetti G, Anversa P (1994) Acute myocardial infarction leads to upregulation of the IGF-1 autocrine system, DNA replication, and nuclear mitotic division in the remaining viable cardiac myocytes. Exp Cell Res 213:463–472
49. Sabbah HN, Sharov VG (1998) Apoptosis in heart failure. Prog Cardiovasc Disease 40:549–562
50. Savill JS, Haslett C (1995) Granulocyte clearance by apoptosis in the resolution of inflammation. Semin Cell Biol 6:385–393
51. Savill JS, Wyllie AH, Henson JE, Walport MJ, Henson PM, Haslett C (1989) Macrophage phagocytosis of aging neutrophils in inflammation: programmed cell death in the neutrophil leads to its recognition by macrophages. J Clin Invest 83:865–875
52. Scherle W (1970) A simple method for volumetry of organs in quantitative stereology. Microskopie 26:57–63
53. Sterio DC (1984) The unbiased estimation of number and sizes of arbitrary particles using the disector. J Microsc 134: 127–136
54. Takaori K, Kim S, Ohta K, Hamaguchi A, Yagi K, Iwao H (1997) Inhibition of nitric oxide synthase causes cardiac phenotypic modulation in rat. Eur J Parmacol 322:59–67
55. Takemura G, Ohno M, Hayakawa Y, Misai J, Kanoh M, Ohno A, Uno Y, Minatoguchi S, Fujiwara T, Fujiwara H (1998) Role of apoptosis in the disappearance of infiltrated and proliferated interstitial cells after myocardial infarction. Circ Res 82:1130–1138
56. Vaux DL, Strasser A (1996) The molecular biology of apoptosis. Proc Natl Acad Sci U S A 93:2239–2224
57. Vyalov S, Desmoulière A, Gabbiani G (1993) GM-CSF-induced granulation tissue formation: relationships between macrophagew and myofibroblast accumulation. Virchows Archiv 63:231–239
58. Weber KT, Brilla CG (1991) Pathological hypertrophy and cardiac interstitium, fibrosis and renin-angiotensin-aldosterone system. Circulation 83:1849
59. Weihrauch D, Zimmermann R, Arras M, Schaper J (1994) Expression of extracellular matrix proteins and the role of fibroblasts and macrophages in repair processes in ischemic porcine myocardium. Cell Mol Biol Res 40: 105–116
60. Williams GT (1991) Programmed cell death: apoptosis and oncogenesis. Cell 65:1097–1098
61. Yu CCW, Filipe MI (1993) Update on proliferation-associated antibodies applicable to formalin-fixed paraffin-embedded tissue and their clinical applications. Histochem J 25:843–853
62. Zar H (1999) Biostatistical analysis. Prentice Hall, Upper Saddle River, p 663